J. Astrophys. Astr. (2018) 39:37
https://doi.org/10.1007/s12036-018-9531-8

Numerical simulation of inertial alfven waves to study localized structures and spectral index in auroral region

BHEEM SINGH JATAV

Department of Physics, Sikkim University, Gangtok, Sikkim 737101, India.
E-mail: bheemsinghj@gmail.com

MS received 10 March 2018; accepted 21 May 2018; published online 7 June 2018

Abstract. In the present paper, the numerical simulation of Inertial Alfven wave (IAW) in low-β plasma applicable to the auroral region at 1700 km was studied. It leads to the formation of localized structures when the nonlinearity arises due to ponderomotive effect and Joule heating. The effect of perturbation and magnitude of pump IAW, formed the localized structures of magnetic field has been studied. The formed localized structures at different times and average spectral index scaling of power spectrum have been observed. Results obtained from simulation reveal that spectrum steepens with power law index ~ -3.5 for shorter wavelength. These localized structures could be a source of particle acceleration and heating by pump IAW in low-β plasma.

Keywords. Inertial Alfven wave—auroral—plasma.

1. Introduction

Alfven waves have been extensively studied because of their importance both in space and laboratory plasma – such as auroral ionosphere (Stasiewicz *et al.* 2000), solar coronal plasma heating (Shukla *et al.* 2006), extended corona heating by ions (Wu & Yang 2007), etc. (space plasma) and tokamak plasma heating (Vlad *et al.* 1999), large plasma devices (Carter & Dorfman 2014), etc. (laboratory plasma). The dispersion relations of Alfven wave have been obtained from MHD equation, which is non-dispersive (Alfven 1942), but because of their finite frequency and electron inertial force along magnetic field in plasma, Alfven waves become dispersive in nature (Hasegawa 1976). Alfven waves have been observed by Freja, FAST, Polar, Cluster spacecraft in space plasma (Chaston *et al.* 1999). Alfven waves become dispersive inertial and kinetic Alfven waves. The dispersion of the inertial Alfven wave comes from the parallel electron inertia. Dispersive inertial Alfven waves are evoked to explain particle acceleration and heating (Seyler & Liu 2007), ponder-motive density (Dasgupta *et al.* 2003), wave–particle interaction (Voitenko & Goossens 2005), the formation of localized structures (Sundkvist *et al.* 2007) and energy transportation from one source to another in the space plasma like auroral regions (Chaston *et al.* 2008).

The parallel phase speed of the IAW is much larger than the electron thermal speed, so that the IAW appear in uniform magnetosplasma with $\beta << m_e/m_i$ (electron to ion mass ratio), where m_e and m_i are the electron and ion mass, $\beta = 8\pi n_{e0} T/B_0^2$ (thermal to magnetic pressure ratio), n_{e0} is the unperturbed electron number density, T_e is the electron temperature, and B_0 is the external magnetic field (Shukla & Stenflo 1999a). Due to the non-zero parallel electric field and density perturbation, IAW could be a responsible for particle acceleration.

In the literature, Shukla *et al.* (1996) and Shukla & Stenflo (1997) explained the inertial Alfven waves can driven by equilibrium sheared plasma flows, which produced the large amplitude inertial Alfven waves. Hasegawa & Uberoi (1982) and Shukla & Stenflo (1995) shows the finite amplitude inertial Alfven waves can produce a nonlinear effect. Shukla & Stenflo (1999b) considered the nonlinear interaction between large-amplitude dispersive inertial Alfven waves (DIAW) and electrostatic density perturbations to studied the modulational instability of constant amplitude DIAW. They also pointed out that possibility of DIAW induced quasi-stationary (supersonic) density channels (cavities). Kumar *et al.* (2011) numerically studied the model equation governing the nonlinear interaction between the dispersive Alfven wave and magnetosonic wave in the low- β plasma. They also explain the investigation to low-β plasma in solar corona and auroral ionospheric plasma. Sharma *et al.* (2015) studied the nonlinear evolution of three-dimensional propagating inertial Alfven waves in the presence of background density fluctuation for low-β plasma. The recent various studies of nonlinear phenomena of Alfven waves have been established from the kinetic to inertial regime in numerous laboratory observations and theoretical analysis (Carter *et al.* 2006; Zhao *et al.* 2015). But the nonlinear process of particle heating and acceleration is not well understood. Thus, the nonlinear phenomenon of Alfven waves for low-β plasma becomes open research problem in the plasma physics (Rinawa *et al.* 2015). Until now have not been studied the effect of magnitude of pump IAW on localized structures and power spectral index for low-β plasma.

The prime objective of this paper to study the magnitude and nonlinear effect associated with the finite frequency of pump IAW for low-β plasma on the formation of localized structures and turbulent spectrum applicable to the auroral region at 1700 km. To investigate the these effect, the modified dynamical equation of IAW have been derived. This effect has been studied by numerical methods. The paper layout is as follows. Section 2 consists the brief review of model equation for IAW and section 3 presents numerical simulation. The results, discussion and conclusion are in section 4.

2. Model equation

We consider the dynamics of low-frequency, long-wavelength, finite amplitude IAW, where the ambient magnetic field is along the z-axis., i.e. $\vec{B}_0 = B_0\hat{z}$, and B_0 is the background magnetic field. The propagation of waves in the x-z plane, i.e. $\vec{k} = k_x\hat{x} + k_z\hat{z}$. Therefore, the dynamical equation for IAW for low-β plasma can be obtained by using the standard method (Shukla & Stenflo 1999a; Shukla *et al.* 1999; Shukla & Stenflo 2000a; Shukla & Sharma 2002) and can be written as

$$\frac{\partial^2 B_y}{\partial t^2} - \lambda_e^2 \frac{\partial^4 B_y}{\partial x^2 \partial t^2} + v_A^2\left(1 - \frac{\delta n_s}{n_0}\right)\frac{\partial^2 B_y}{\partial z^2}, \quad (1)$$

where $v_A(=\sqrt{B_0^2/4\pi n_0 m_i})$ is the Alfven speed, $\lambda_e(=\sqrt{c^2 m_e/4\pi n_0 e^2})$ is the collision-less electron skin depth, $\delta n_s = n_e - n_0$ is the number density change due to the low-frequency IAW, and n_e and n_0 are are the modified and unperturbed plasma number densities. If we consider only the effect of finite parallel electron inertia and neglect the effect of perpendicular ion inertia, then the dispersion relation of Eq. (1) is written (Shukla & Stenflo 2000b) as follows:

$$\frac{\omega^2}{k_{0z}^2 v_A^2} = \frac{1}{1 + k_{0x}^2\lambda_e^2} \quad (2)$$

Consider the solution of Eq. (1) as given below

$$B_y = \tilde{B}_y(x, z, t)e^{i(k_{0x}x + k_{0z}z - \omega t)} \quad (3)$$

Substituting Eq. (3) into Eq. (1) and simplifying dynamical equation, for the case $\partial_z \tilde{B}_y << k_{0z}\tilde{B}_y$, we get

$$-2i\omega(1 + \lambda_e^2 k_{0x}^2)\frac{\partial \tilde{B}_y}{\partial t} - 2ik_{0z}v_A^2\frac{\partial \tilde{B}_y}{\partial z} - v_A^2\frac{\partial^2 \tilde{B}_y}{\partial z^2} - \lambda_e^2\omega^2\frac{\partial^2 \tilde{B}_y}{\partial x^2} + 2ik_{0x}\lambda_e^2\omega^2\frac{\partial \tilde{B}_y}{\partial x} - k_{0z}^2 v_A^2\frac{\delta n_s}{n_0}\tilde{B}_y = 0 \quad (4)$$

where $k_{0x}(k_{0z})$ is the component of wave vector perpendicular (parallel) to $\hat{z}B_0$, and ω_0 is the inertial Alfven wave frequency.

The density can be modified due to both Joule heating and the ponderomotive force for low-β plasma; on the other hand, consider the small density fluctuation due to electron parallel inertia for IAW (Shukla & Stenflo 1999a) as follows:

$$\frac{\delta n_s}{n_0} \approx (-\xi|\tilde{B}_y|^2) \quad (5)$$

where $\xi = (1 + 8k_{0x}^2\lambda_e^2)/48\pi n_0 T_e$.

Using Eq. (5) and rewriting Eq. (4) in dimensionless form,

$$-i\frac{\partial \tilde{B}_y}{\partial t} + i\Delta\frac{\partial \tilde{B}_y}{\partial x} + \frac{\partial^2 \tilde{B}_y}{\partial x^2} - i\frac{\partial \tilde{B}_y}{\partial z} - \frac{\partial^2 \tilde{B}_y}{\partial z^2} + |\tilde{B}_y|^2\tilde{B}_y = 0 \quad (6)$$

Further we can modify Eq. (6) for the modulation instability of plasma, which is saturable self-focusing in nonlinear media (Zakharov & Shabat 1972; Cap 1978; Akhmediev *et al.* 1990; Zhou *et al.* 1994; Knudsen 1996) as

$$-i\frac{\partial \tilde{B}_y}{\partial t} + i\Delta\frac{\partial \tilde{B}_y}{\partial x} + \frac{\partial^2 \tilde{B}_y}{\partial x^2} - i\frac{\partial \tilde{B}_y}{\partial z} - \frac{\partial^2 \tilde{B}_y}{\partial z^2} + \frac{|\tilde{B}_y|^2}{1 + g|\tilde{B}_y|^2}\tilde{B}_y = 0 \quad (7)$$

where $\Delta = 2k_{0x}\lambda_e\omega/k_{0z}v_A$ is the parameter in terms of electrons collision-less skin depth, g is the magnitude of pump wave amplitude.

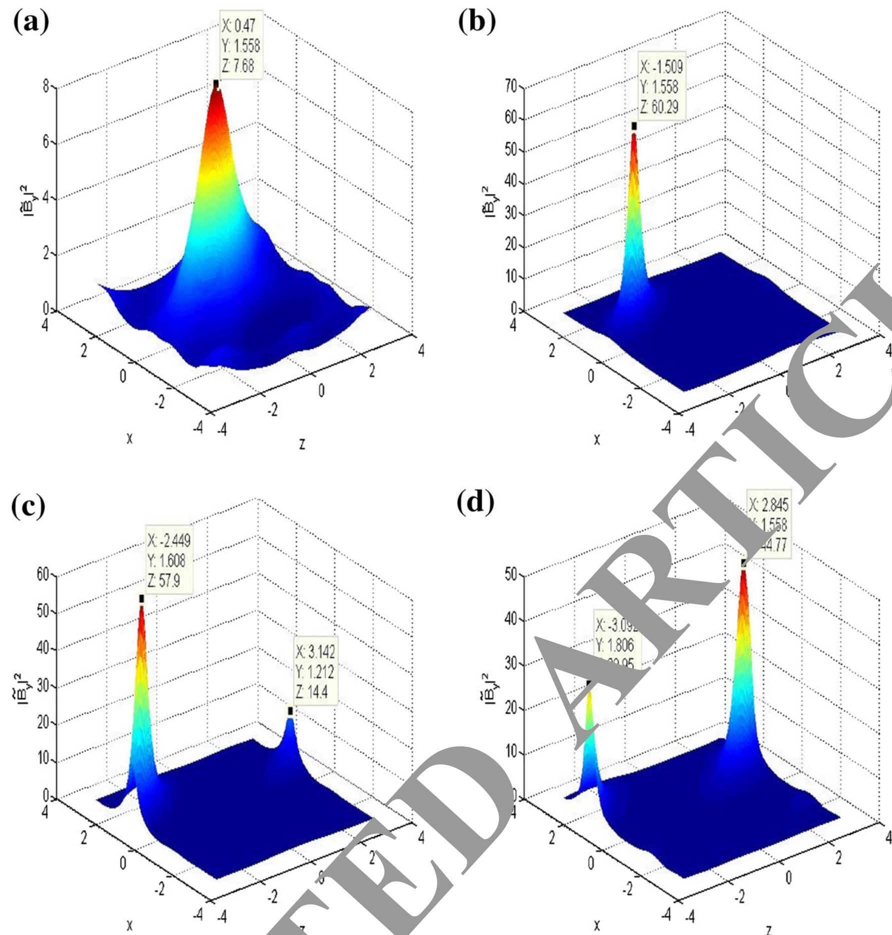

Figure 1. The magnetic field intensity profile of IAW for low-β plasma like auroral region at (**a**) $t = 13$, (**b**) $t = 15$, (**c**) $t = 16$ and (**d**) $t = 17$.

The normalizing parameters are

$x_N \approx \lambda_e\omega_0/k_{0x}v_A$, $z_N \approx 1/k_{0z}$,
$t_N \approx 2\omega_0(1 + k_{0x}^2\lambda_e^2)/k_{0z}^2 v_A^2$,
$B_N \approx 1/\sqrt{(1 + 8k_{0x}^2\lambda_e^2)/48\pi n_0 T_e}$.

When the second term in Eq. (7) vanishes along with $g = 0$, then Eq. (7) reduces to NLSE. When $\Delta = 0$, the solution to be considered by Zhou *et al.* (1994) of Eq. (7).

3. Numerical simulation

Numerical solution to Eq. (7) was obtained using the two-dimensional pseudo-spectral method. The simulation was carried out with (128 × 128) grid points in a periodic spatial domain of $(2\pi/\alpha_x) \times (2\pi/\alpha_z)$ with $\alpha_x, \alpha_z = 1$. The initial conditions for the simulation were

$$\tilde{B}_y(x, z, 0) = |a_0|[1 + 0.1\cos(\alpha_x x)][1 + 0.1\cos(\alpha_z z)] \tag{8}$$

where $|a_0| = 1$ is the initial amplitude of the homogeneous pump IAW.

The finite-difference method with a predictor–corrector scheme was used for the integration in the time domain with a time step of $dt = 5 \times 10^{-4}$. Before solving Eq. (7) numerically, we wrote the algorithm for 2D cubic NLSE. The precision of computation is monitored by plasma consistency number, $N = \sum_k |B_k|^2$ when g = 0 and $\Delta = 0$, which have been maintained up to the order of 10^{-5} in the simulation. After testing this algorithm, we wrote a modified algorithm for case $g \neq 0$ and $\Delta \neq 0$ of Eq. (7). The formation of localized structures of IAW at various times and keeping g (= 0.9) and Δ(= 0.04) fixed are presented as follows.

For application purpose, the typical plasma parameters of aurora at 1700 km altitude (Wu *et al.* 1996) are $B_0 \approx 0.3G$, $n_0 \approx 5 \times 10^3 cm^{-3}$, $T_i \approx T_e \approx 1eV$,

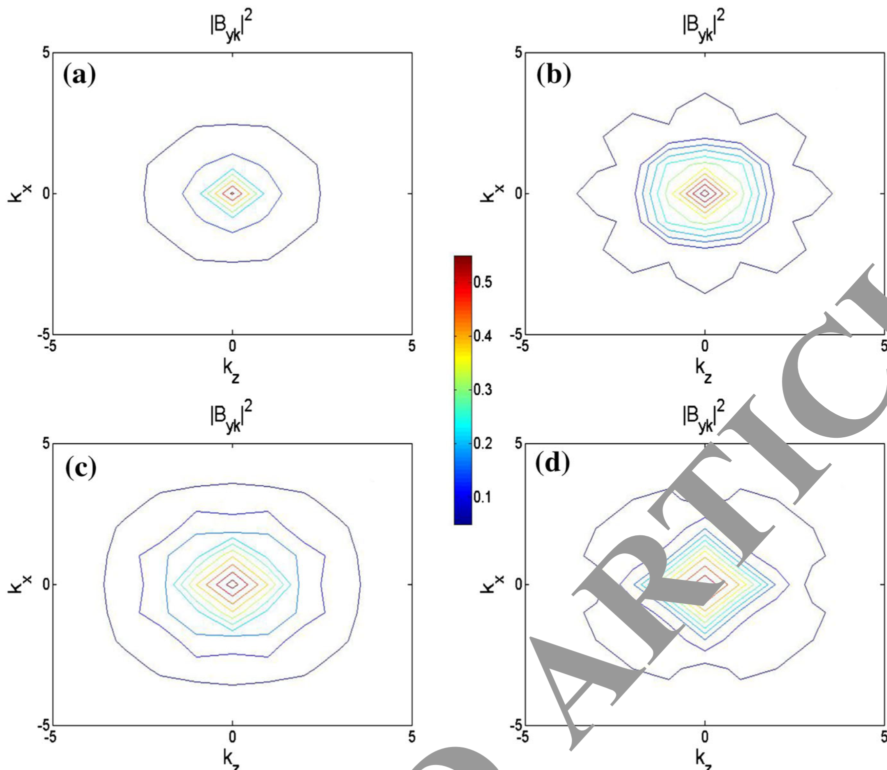

Figure 2. Contour of $|B_{yk}|^2$ against Fourier modes of IAW. (**a**) $t = 13$, (**b**) $t = 15$, (**c**) $t = 16$ and (**d**) $t = 17$.

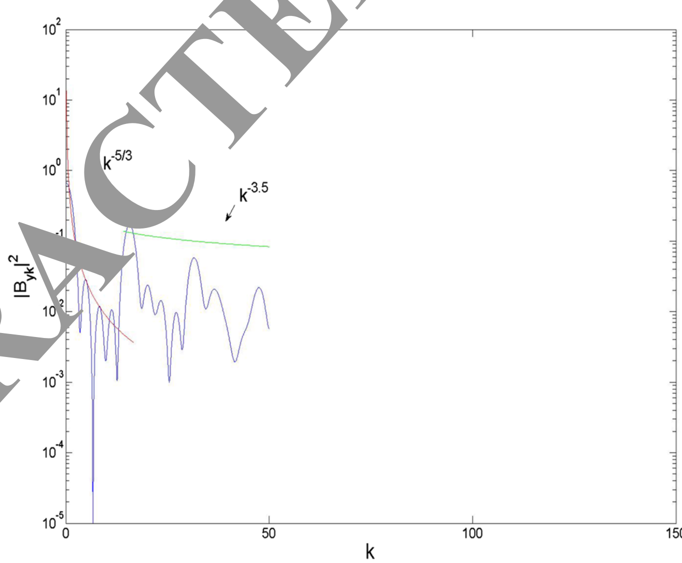

Figure 3. Variation of $|B_{yk}|^2$ against $k_\perp$ at $k_{||} = 0$ of IAW in low-β plasma at $t = 13$.

then $\beta \approx 2.2 \times 10^{-6}$, $V_{Te} \approx 4.2 \times 10^7 cm/s$, $v_A \approx 9.3 \times 10^8 cm/s$, $\omega_{ci} \approx 2.9 \times 10^3 Hz$, $\lambda_e \approx 7.5 \times 10^3 cm$. For these parameters at $\omega_0/\omega_{ci} \approx 0.04$ and $k_{0x}\lambda_e \approx 0.02$, we get $k_{0x} \approx 3.1 \times 10^{-6} cm^{-1}$, $k_{0z} \approx 1.24 \times 10^{-7} cm^{-1}$. The values of normalizing parameters are $x_N \approx 3.01 \times 10^2 cm$, $z_N \approx 8.06 \times 10^6 cm$. $t_N \approx 0.02s$, $B_N \approx 866.7G$, $\Delta \approx 0.04$.

Here, the simulation results of IAW for low-β plasma are presented at four instants time namely $t = 13$, 15, 16, 17, where the magnitude of pump wave amplitude has been fixed. Figure 1 depicts the formation of nonlinear localized structures at four instant times ($t = 13$, 15, 16, 17). It is evident from figure that the localized structures are formed at different times with different amplitude $|\tilde{B}_y|^2$. Figure 1(a) depicts one localized structure at one location having amplitude $|\tilde{B}_y|^2 \sim 7.68$ at t = 13. Figure 1(b) depicts one localized structures at different location having different amplitude $|\tilde{B}_y|^2 \sim 60.29$ at t = 15. Further, if we take higher time at $t = 16$ (Fig. 1(c)), then the pattern is found two at different location and having different intensity $|\tilde{B}_y|^2 \sim 57.9, 14.4$, with greater difference. Figure 1(d) depicts again two localized structure having intensity $|\tilde{B}_y|^2 \sim 29.95, 44.77$ at time $t = 17$, which is less intensity from $t = 16$. At early times, less intense localized structures are formed. With advancement of time these structures are more intense and complex are found (Fig. 1(c) and (d)) and the system reaches its quasi-steady state.

Figure 2(a–d) depict the contour plots of spectra of $\tilde{B}_y$ in the (k_z, k_x) Fourier space at four instant times namely t = 13, 15, 16, 17. Figure 2(a) shows the most intense localized structure and at the advancement of time we found more chaotic localized structures (Fig. 2(b)–(d)). These structures show that if we increase the time, the location of the localized structures vary and become more chaotic structures.

Next, we studied the average power spectral index at time $t = 13$ as depicted in Fig. 3, which shows the variation of $|B_{yk}|^2$ against $k_\perp$ for the fixed value of $k_{||}$. It is evident from the wave number spectrum that $k_z\lambda_e < 1$ the spectral index is near the Kolmogorov $k^{-5/3}$ scaling (inertial range scaling). A turbulent spectra breakup at $k_\perp\lambda_e \approx 1$. Earlier Chaston *et al.* (2006) and Lund (2010) studied the inertial range of power spectra based on space craft data. For wave number spectrum at $k_\perp\lambda_e > 1$, the average power spectrum becomes steeper with power low index $\sim k^{-3.5}$, which is consistent studied by Kintner (1976) and Gurnett *et al.* (1984). Further, also from Fig. 3, steepening of the turbulence power spectrum is consistent with the result reported from the analysis of the data recorded by the HEOS 2, Hawkeye 1, and the Dynamics Explorer 1 spacecraft for auroral region (Kitner 1976; Gurnett *et al.* 1984; Lund 2010).

Therefore, the formation of localized structure and power spectral index of turbulence are important for the heating and particle acceleration in auroral region. Various authors studied the IAW are responsible for solar heating and particle acceleration in the auroral region (Marklund *et al.* 1994, 1995; Shukla *et al.* 2006). Still, it is a challenge to understand the heating and particle acceleration in auroral region. This investigation reveals that the formation of localized structures and power spectral index has been affected by the magnitude of finite frequency pump IAW.

4. Summary and conclusion

For the auroral region parameters, we carried out the numerical simulation of Eq. (7), representing the dynamics of finite frequency IAW in low-β plasma, for the fixed magnitude of pump IAW. The formation of localized structure and power spectral index changed by changing time at the fixed magnitude of pump IAW. From the initialization of time, localized structures are formed. But when time advancement is taken, the location and intensity of structures change and form more chaotic structures. Further, from the obtained result, we found that for $k_\perp\lambda_e < 1$, the spectral index follows $(k^{-5/3})$ the Kolmogorov scaling (scaling shows by read line) and for $k_\perp\lambda_e > 1$ the steeper spectral index follows $(k^{-3.5})$(scaling shows by green line) for finite frequency of IAW and the system reaches its quasi-steady state. The steepening of spectral index of IAW may heat and accelerate plasma particle in auroral region, consistent with the result observed by Gurnett *et al.* (1984) and Chaston *et al.* (2004). Hence, the magnitude of finite frequency pump IAW affects the localized structures and power spectral index of IAW, which are responsible for heating and acceleration of particles in low-β plasma, such as auroral regions.

Acknowledgements

This work was supported by RGNF, UGC, India. This work also partially supported by DST, India.

References

Alfven H. 1942, Nature, 150, 405
Akhmediev N. N., Heatley D. R., Stegeman G. I., Wright E. M. 1990, Phys. Rev. Lett., 65, 1423
Cap F. F. 1978, Handbook on plasma Instabilities, 1st edition, Academic Press, P. 623
Carter T., Dorfman S., 2014, URSI General Assembly and Scientific Symposium, IEEE Conference, Volume 5, p. 3216
Carter T. A., Brugman B., Pribyl P., Lybarger W. 2006, Phys. Rev. Lett., 96, 155001
Chaston C. C., Bonnell J. W., Carlson C. W., McFadden J. P., Ergun R. E., Strangeway R. J., Lund E. J. 2004, J. Geophys. Res., 109, A04205
Chaston C. C., Carlson C. W., Peria W. J., Ergun R. E., McFadden J. P. 1999, Geophys. Res. Lett., 26, 647
Chaston C. C., Genot V., Bonnell J. W., Carlson C. W., McFadden J. P., Ergun R. E., Strangeway R. J., Lund E. J., Hwang K. J. 2006, J. Geophys. Res., 111, A03206

Chaston C. C., Salem C., Bonnell J. W., Carlson C. W., Ergun R. E., Strangeway R. J., McFadden J. P. 2008, Phys. Rev. Lett., 100, 175003

Dasgupta B., Tsurutani B. T., Janaki M. S. 2003, Geophys. Res. Lett., 30, 2128

Gurnett D. A., Huff R. L., Menietti J. D., Burch J. L., Winningham J. D., Shawhan S. D. 1984, J. Geophys. Res., 89, 8971

Hasegawa A. 1976, J. Geophys. Res., 81, 5083

Hasegawa A., Uberoi C., 1982, The Alfven Wave, Technical Information Center U. S. Department of Energy

Kintner Jr. P. M. 1976, J. Geophys. Res., 81, 5114

Knudsen D. J. 1996, J. Geophys. Res., 101, 10761

Kumar S., Sharma R. P., Singh H. D. 2011, Solar physics, 270, 523

Lund E. J. 2010, J. Geophys. Res., 115, A01201

Marklund G., Blomberg L., Falthammar C.-G., Lindqvist P.-A. 1994, Geophys. Res. Lett., 21, 1859

Marklund G., Blomberg L., Falthammar C.-G., Lindqvist P.-A., Eliasson L. 1995, Ann. Geophys., 13, 704

Rinawa M. L., Gaur N., Sharma R. P. 2015, Phys. Plasmas, 22, 022310

Seyler C. E., Liu K. 2007, J. Geophys. Res, 112, A09302

Shukla P. K., Stenflo L. 1995, Phys. Scr., T60, 32

Shukla P. K., Stenflo L. 1997, Phys. Plasmas, 4, 3445

Shukla P. K., Stenflo L. 1999a, Phys. Plasmas, 6, 4120

Shukla P. K., Stenflo L. 1999b, Phys. Plasmas, 6, 1677

Shukla P. K., Stenflo L. 2000a, Phys. Plasmas, 7, 2738

Shukla P. K., Stenflo L. 2000b, Phys. Plasmas, 7, 2747

Shukla A., Sharma R. P. 2002, J. Geophys. Res., 107, 1338

Sharma R. P., Kumari A., Yadav N. 2015, Phys. Plasmas, 22, 112303

Shukla P. K., Stenflo L., Bingham R. 1999, Phys. Plasmas, 6, 1677

Stasiewicz K., Bellan P., Chaston C., Kletzing C., Lysak R., Maggs J., Pokhotelov O., Seyler C., Shukla P., Stenflo L., Streltsov A., Wahlund J. E. 2000, Space Sci. Rev., 92, 423

Sundkvist D., Retino A., Vaivads A., Bale S. D. 2007, Phys. Rev. Lett., 99, 025004

Shukla P. K., Bingham R., Eliasson B., Dieckmann M. E., Stenflo L. 2006, Plasma Phys. Control. Fusion, 48, B249-B255

Shukla P. K., Birk G. T., Dreher J., Stenflo L. 1996, Plasma Phys. Rep., 22, 818

Voitenko Y., Goossens M. 2005, Phys. Rev. Lett., 94, 135003

Vlad G., Zonca F., Briguglio S. 1999, Riv. Nuovo Cim., 22, 1

Wu D. J., Yang L. 2007, Astrophys. J., 659, 1693

Wu D. J., Huang G. L., Wang D. Y. 1996, Phys. Rev. Lett., 77, 4346

Zakharov V. E., Shabat A. B. 1972, Sov. Phys. JETP., 34, 1

Zhao J. S., Voitenko Y., Keyser J. D., Wu D. J. 2015, Astrophys. J., 799, 222

Zhou C., He X. T., Cai T. 1994, Phys. Rev. Lett., 50, 5